JOURNAL OF SOLID STATE CHEMISTRY 30, 311–319 (1979)

The Thallium Tungstate $Tl_2W_4O_{13}$: A Tunnel Structure Related to the Hexagonal Tungsten Bronze

M. GOREAUD, PH. LABBE, J. C. MONIER, AND B. RAVEAU

Laboratoire de Cristallographie et Chimie du Solide, Laboratoire associé au CNRS n° 251, Université de Caen, 14032 Caen Cedex, France

Received October 5, 1978; in final form January 22, 1979

The crystal structure of thallium tungstate $Tl_2W_4O_{13}$ ($a = 7.327$ Å; $b = 37.864$ Å; $c = 3.840$ Å; space group *Pmab*) has been resolved by three-dimensional single-crystal X-ray analysis. The average structure was resolved by standard Patterson and Fourier techniques and refined by full-matrix least squares to final agreement indices $R = 0.087$ and $R_w = 0.100$. Superstructure reflections referred to a supercell (a, b, $2c$; space group *Pcab*) led to a framework model which is described. The structure consists of corner-sharing chains of WO_6 octahedra parallel to a and c axes. Hexagonal and pentagonal tunnels, bound by these chains, are filled by thallium atoms. The atomic arrangement is closely related to the hexagonal bronze structure. The tungstate $Tl_2W_4O_{13}$ can thus be considered as a member of a series of phases $(TlB_3X_9)_n \cdot Tl_6B_{10}X_{34}$ (X = O, F) involving hexagonal tungsten bronze ribbons.

Introduction

As shown in a recent review (*1*), the structure of hexagonal tungsten bronze (HTB) A_xWO_3, first described by Magneli (*2*), can be considered as the starting point of several oxide families. Hence, the thallium tungstate $Tl_2W_4O_{13}$ isolated by Shivahare (*3*) is of some interest. The relationship with HTB was first shown by Michel (*4*); the lattice is orthorhombic with cell parameters $a = 7.30$ Å, $b = 37.9$ Å, and $c = 7.67$ Å. They are related to those of the HTB a_H and c_H in the following manner: $a \sim a_H$, $b \sim 3a_H 3^{1/2}$, and $c \sim c_H$. To our knowledge, the structural relationships between this oxide and the bronze Tl_xWO_3 have not been explained. We present here the results of our investigations on the structure of $Tl_2W_4O_{13}$. This differs from the bronze Tl_xWO_3 in possessing a large excess of oxygen and thallium atoms.

Preliminary Studies

Synthesis of the Crystals

$Tl_2W_4O_{13}$ crystals were prepared from a mixture of thallium carbonate Tl_2CO_3 and tungsten oxide WO_3 in the molar ratio 1:4. In the first stage the mixture was heated at 300°C to decompose the Tl_2CO_3. The temperature was raised slowly up to 500°C and maintained there for 3 to 4 hr. Finally, the crystals were obtained after heating for about 12 hr at 650–700°C. The crystals were transparent and needle shaped with a thickness of only a few tens of micrometers. An extinction between crossed polaroids was observed in the longitudinal direction.

Intensity Measurements

The first Weissenberg photographs, taken with Cu$K\alpha$ radiation for different samples, showed diffuse streaks, indicating crystals of poor quality. Effectively, observed streaks

0022-4596/79/120311-09$02.00/0

are related to strong spots, and their most frequent orientations are normal to the [*hkl*] directions. These features are more or less pronounced for the studied samples, which suggest that they are not in relation with a systematic disorder in this type of structure. From among the samples chosen for their thinness in order to minimize absorption, we selected those for which the diffuse scattering was the weakest. Four crystals were studied; for one of them (No. 1), registered with Cu$K\alpha$ radiation using a photographic technique, the intensities of 755 independent reflections were measured by microphotometry. The spectra of the other three were registered, for Mo$K\alpha$ radiation, using a CAD 4 Enraf Nonius single-crystal diffractometer. Crystal No. 2 was a square section parallelepiped (8×8 μm). It became apparent later that the small diffraction volume strongly limited the number of reflections (635 independent *hkl*). In the case of crystal No. 3 (approx $12\times30\times840$ μm), the data were collected for one-fourth of the sphere of reflection up to $2\theta = 82°$ using the ω–2θ technique with a maximum scanwidth of 1.30° and a counter slit aperture of 3.70 mm. The background intensity was measured on each side of the reflection. A systematic control on three reflections did not indicate any anomalous function during the experiment. A total of 8059 reflections, collected with a program which optimizes the transmission factors, were corrected for absorption phenomena, assuming a cylindrical crystal. The number of reflections was reduced to 1637 with $I > 3\sigma(I)$ after comparison of equivalent sectors. The correction for Lorentz and polarization effects was applied. Only 620 reflections had an intensity greater than one one-hundredth of the strongest. Moreover, 850 superstructure reflections were also registered and verified using the Weissenberg technique. The intensities of these were less than 3% of the strongest. These reflections were not included in the refinements of the average structure. Crystal No. 4 ($24\times8\times400$ μm), which exhibited few diffuse streaks, has been treated in the same manner in order to verify the different steps of the calculation. In this case, the number of reflections was 1232.

Symmetries and Space Groups

A hexagonal sublattice was deduced from the analysis of the Laue patterns, but the intensities measured in the equivalent sectors show that the orthorhombic symmetry is confirmed. The cell parameters based on 25 reflections and refined by the method of least squares are $a = 7.327(2)$ Å, $b = 37.864(5)$ Å, and $c = 3.840(1)$ Å. Systematic absences observed for $h0l$, $h = 2n+1$, and $hk0$, $k = 2n+1$, led for the average structure to the space groups *Pmab* or $P2_1ab$. Statistical tests, applied to the distribution of the normalized structure factors, did not allow elimination of one of these groups. The uncertainty could be removed by studying the superstructure reflections. The latter were indexed in an orthorhombic system ($a'b'c'$) corresponding to the relationship $a' = a$, $b' = b$, and $c' = 2c$ with the systematic absences $h'0l'$, $h' = 2n+1$; $h'k'0$, $k' = 2n+1$; and $0k'l'$, $l' = 2n+1$. This leads to the unique space group *Pcab*, characterized by 2_1 axis in the three reference directions. The association of this symmetry with the c translation leads for the (*abc*) cell to the unique space group *Pmab* (Fig. 1).

Solution and Refinement of the Structure

The crystal structure was resolved by standard Patterson and Fourier techniques and refined by the full-matrix least-squares method. Atomic scattering factors of W^{6+}, Tl^{+}, and O^{2-} were calculated from values published by Cromer and Waber (*5*) and Suzuki (*6*). Anomalous dispersion corrections for W and Tl were made with values given by Cromer (*7*). A linear weighting

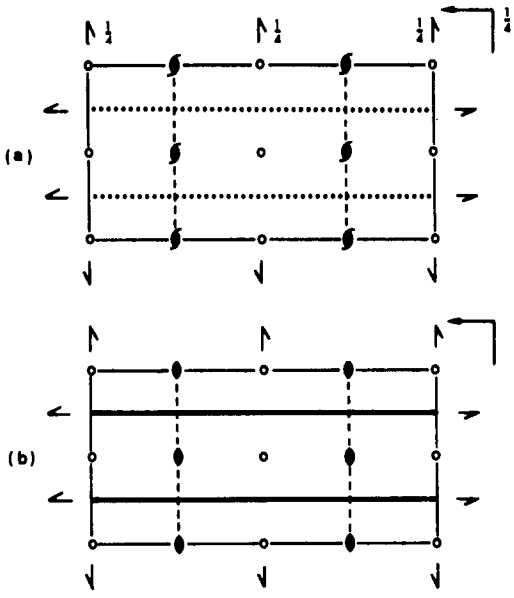

FIG. 1. Space groups. (a) Actual structure with cell $a\times b\times 2c$. Group *Pcab*, standard: *Pbca*. (b) Average structure with cell $a\times b\times c$. Group *Pmab*, standard: *Pbcm*.

scheme was adjusted from a study of the function $\langle w|F_o-F_c|\rangle$ in terms of $\sin\theta/\lambda$.

Heavy Atoms

The arrangement of the five heavy atoms was derived from the three-dimensional Patterson function. Their position in the projection onto (001) is very close to that of a hexagonal lattice (Fig. 2). The scattering factors f_{Tl} and f_W not being very different, the discrimination between the two types of atoms was only possible later in the study. The Tl(1) and Tl(3) atoms are close to the level $z=0$, from which they do not deviate more than 0.22 Å, while the W(4) and W(5) atoms are gathered about $z=\frac{1}{2}$. Only the W(2) atoms have the value $z=0.38$. During the first cycles, these atoms refined correctly except for Tl(3) located in the (100) mirror with $x=0.25$. The high value of $\beta_{11}=0.0466$ obtained for this atom corresponds to a displacement of 0.35 Å. On the other hand, a distribution of Tl(3) on two symmetrical sites, one on each side of the (100) mirror plane which contains Tl(1) and W(2), led to a more reasonable β_{11} value. After the heavy atom refinements, the calculations converged with $R=0.105$ and $R_w=0.118$.

Oxygen Atoms

The difference synthesis was carried out afterward and showed 15 important peaks which could correspond to the nine oxygen atoms of the average structure. The analysis of these positions led us to the conclusion that each of the three oxygen atoms O(7), O(8), and O(9), situated on about the same level as the tungsten atoms, occupied split sites along z separated by about 0.54 Å. The oxygen atoms O(12), O(13), and O(14) which lie approximately above the W(2), W(4), and W(5) atoms (Fig. 2) are distributed between split sites in the (001) plane, separated by a distance of about 0.80 Å. It should be noted that the amount of data obtained from crystal No. 2 did not allow the same accuracy for the oxygen atoms, using the Fourier difference maps, and hence only their average position was obtained. The same result was obtained by limiting the amount of information obtained from crystal No. 3 to the 620 most intense reflections. The above model was refined with an occupancy factor of 0.5 for all the split positions; x and y refined normally for all the atoms. On the other hand, the z coordinate of the oxygen atoms converged weakly. For some of the split oxygen atoms [O(8A), O(9B), and O(14)], the value of z oscillated from one cycle to another. The level z of O(7A) decreased during the last three cycles, while that of O(13B) was fixed up with that of O(13A). The maximum value of the isotropic temperature factors is 1.40. In the last cycle, three of them assumed values close to zero and that of O(12) became negative.

Final atomic parameters and standard deviations are given in Table I. The R factors remain high ($R=0.094$ and $R_w=0.109$ for crystal No. 3 and $R=0.087$, $R_w=0.100$ for No. 4) due to the poor quality of the crystals.

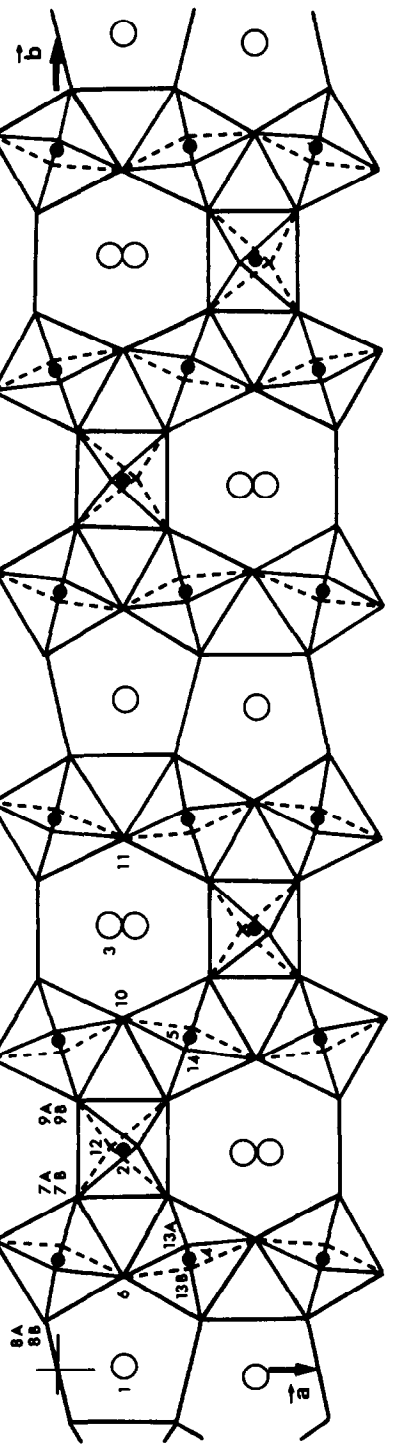

FIG. 2. $Tl_2W_4O_{13}$. Projection of the structure onto (001). Only one layer of $[WO_6]$ octahedra is drawn.

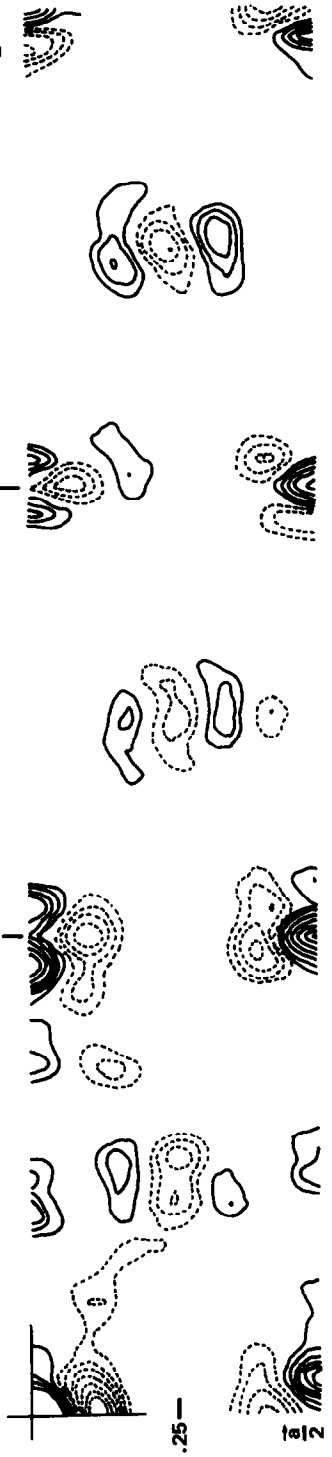

FIG. 3. Section $z=0$ of the Patterson's partial function calculated with superstructure reflections. Solid lines represent positive peaks, broken lines represent negative peaks.

TABLE I

ATOMIC PARAMETERS[a] AND STANDARD DEVIATIONS FOR THE AVERAGE STRUCTURE

	x	y	z	β_{11}	β_{22}	β_{33}	β_{12}	β_{13}	β_{23}
Tl(1)	0.25	0.00440(9)	0.0586(7)	0.0082(4)	0.00045(2)	0.0236(12)	0	0	−0.00006(12)
W(2)	0.25	0.16574(6)	0.3845(4)	0.0028(2)	0.00009(1)	0.0048(5)	0	0	−0.00005(9)
Tl(3)	0.2155(5)	0.33484(19)	−0.0249(12)	0.0085(6)	0.00072(3)	0.0374(19)	0.00063(11)	0.0029(7)	0.00046(29)
W(4)	0.5059(2)	0.08219(4)	0.5095(5)	0.0018(1)	0.00017(1)	0.0033(4)	0.00013(3)	−0.0003(3)	0.00031(4)
W(5)	0.5	0.25	0.5248(6)	0.0079(3)	0.00024(1)	0.0021(7)	−0.00095(6)	0	0
O(6)	0.25	0.0711(12)	0.4261(116)	1.17(53)					
O(7A)	0.0547(80)	0.1328(15)	0.5191(110)	0.24(40)					
O(7B)	0.0730(85)	0.1318(16)	0.3691(136)	0.70(56)					
O(8A)	−0.0508(78)	0.0374(16)	0.5137(132)	0.59(47)					
O(8B)	−0.0611(85)	0.0367(17)	0.3682(154)	0.09(37)					
O(9A)	0.0760(78)	0.2031(16)	0.5360(187)	0.06(37)					
O(9B)	0.0740(87)	0.2047(16)	0.3733(128)	0.58(54)					
O(10)	0.25	0.2655(12)	0.4277(120)	1.05(52)					
O(11)	0.25	0.3983(12)	0.4516(113)	0.99(48)					
O(12)	0.1933(73)	0.1694(18)	−0.0806(136)	−0.10(32)					
O(13A)	0.4889(80)	0.0953(15)	−0.0157(173)	1.01(58)					
O(13B)	0.5096(81)	0.0793(15)	−0.0157(173)	1.40(81)					
O(14)	0.4883(81)	0.2414(15)	−0.0448(124)	1.20(71)					

[a] Anisotropic thermal parameters of the form $\exp(-\beta_{ij}h_ih_j)$.

The reflections characterized by a large difference between F_0 and F_c did not show any systematic distribution. Structure factor tables have been deposited.[1]

Superstructure

It was important to verify if the splitting phenomenon was correlated with the doubling of the "c" parameter and could be explained by the existence of the superstructure.

Patterson's partial function was then calculated using only the superstructure reflections. A section, $z = 0$, of this function is shown in Fig. 3. We can see that the largest positive and negative peaks always correspond to the interatomic vectors Tl–Tl. Thus, the pairs of peaks close to the origin or to the point with coordinates (0.5, 0.16, 0) agree reasonably well with the splitting proposed for Tl(3). In the actual structure, this atom would be located in sites compatible with the c (100) mirror with the x coordinate sometimes greater, sometimes smaller than 0.25. Since the Tl(1) atoms have no influence on the superstructure, the curves observed for $x = 0$ and those for a lower peak height, close to $x = 0.25$, could be assigned to Tl(3)–oxygen interatomic vectors and interactions among O(12), O(13), and O(14).

In fact the observed symmetry does not impose any constraint upon the atoms. In the actual cell (Fig. 1a) all the atoms are in general positions and none of them is located on a symmetry center. Two atoms of the same kind, for which the sites are joined by the **c** translation vector, can play a part in the superstructure formation providing the anisotropic thermal motion does not cause the superposition of the vibration ellipsoids. This is very likely the case for the tungsten atoms. On the other hand, the pairs of atoms O(7A)–O(7B), O(8A)–O(8B), and O(9A)-O(9B), displaced along z, make a contribution to the superstructure intensities.

Due to the poor quality of the crystals, atomic positions cannot be obtained more accurately. These observations, however, confirm the importance of Tl(3) and oxygen atoms in the superstructure.

Description of the Structure

The structure is shown in Fig. 2, projected onto the (001) plane. The host lattice is built up of corner-shared [WO_6] octahedra, forming puckered chains with the average directions [100] and [001]. Along **a**, these chains, which include W(4) or W(5), consist of almost regular octahedra tilted sometimes in one direction and sometimes in the other about the axis joining two opposite corners of the octahedron. Thus, the [W(4)] octahedron is rotated by about 9° around the axis passing through O(6). The [W(5)] octahedron is rotated by about 10° around an axis passing through O(10). These rotations cause puckering of the chains along **c**. The chains are linked together by a row of [W(2)] octahedra. These octahedra are rotated by 12.5° about the axis which is parallel to [010] and passes through the middle of two opposite edges. The chains parallel to [001], including W(2) and W(5), are built up of symmetrically equivalent octahedra; that containing W(4) is built up of independent alternating octahedra [W(4)] and [W(4′)]. The interatomic distances in these four types of octahedra are given in Table II. The W–O distances range from 1.73(6) to 2.10(5) Å, except the two distances W(5)–O(14) and W(5)–O(14′) related to the O(14) position which oscillates during the last refinements. The shortest O–O distances (2.52–2.57 Å)

[1] See NAPS document No. 03462 for 5 pages of supplementary material. Order from ASIS/NAPS c/o Microfiche Publications, P.O. Box 3513, Grand Central Station, New York, New York 10017. Remit in advance for each NAPS Accession number. Institutions and organizations may use purchase orders when ordering, however, there is a billing charge for this service. Make checks payable to Microfiche Publications. Photocopies are $5.00. Microfiche are $3.00. Outside of the U.S. and Canada, postage is $3.00 for a photocopy or $1.50 for a fiche.

TABLE II

INTERATOMIC DISTANCES (Å) AND STANDARD DEVIATIONS

W(2) Octahedron		W(5) Octahedron	
W(2)–O(7A)	1.967(57)	W(5)–O(9A)	1.862(60)
–O(7B)	1.827(62)	–O(9B)	1.891(60)
–O(9A)	1.991(60)	–O(10)	1.959(16)
–O(9B)	1.960(62)	–O(10′)	1.959(16)
–O(12)	1.839(52)	–O(14)	1.687(48)
–O(12′)	2.100(52)	–O(14′)	2.213(48)
O(12)–O(7A)	2.87(7)	O(14)–O(9B)	2.67(7)
–O(7B)	2.82(8)	–O(10)	2.83(6)
–O(9B)	2.78(8)	–O(9A)	2.72(8)
–O(9A)	2.82(9)	–O(10′)	2.80(6)
O(12′)–O(7A)	2.77(8)	O(14′)–O(9B)	2.67(8)
–O(7B)	2.70(8)	–O(10)	2.65(6)
–O(9B)	2.64(8)	–O(9A)	2.70(9)
–O(9A)	2.58(9)	–O(10′)	2.68(6)
O(7A)–O(7B)	2.79(8)	O(9B)–O(10)	2.65(7)
O(7B)–O(9B)	2.76(9)	O(10)–O(9A)	2.70(6)
O(9B)–O(9A)	2.64(9)	O(9A)–O(10′)	2.72(7)
O(9A)–O(7A)	2.67(8)	O(10′)–O(9B)	2.64(7)
W(4) Octahedron		W(4′) Octahedron	
W(4)–O(6)	1.947(10)	W(4′)–O(6)	1.947(12)
–O(7B)	2.038(60)	–O(7A)	1.967(57)
–O(8A)	1.728(61)	–O(8B)	1.851(64)
–O(11)	1.948(18)	–O(11)	1.948(18)
–O(13A)	1.894(65)	–O(13A)	2.081(65)
–O(13B)	2.020(52)	–O(13B)	1.827(52)
O(13A)–O(6)	2.91(6)	O(13B)–O(6)	2.88(6)
–O(8A)	2.88(8)	–O(8B)	2.89(8)
–O(11)	2.81(7)	–O(11)	2.83(7)
–O(7B)	2.77(8)	–O(7A)	2.74(8)
O(13B)–O(6)	2.57(6)	O(13A)–O(6)	2.60(7)
–O(8A)	2.60(8)	–O(8B)	2.72(9)
–O(11)	2.65(6)	–O(11)	2.63(7)
–O(7B)	2.55(8)	–O(7A)	2.52(8)
O(6)–O(8A)	2.57(6)	O(6)–O(8B)	2.64(7)
O(8A)–O(11)	2.85(7)	O(8B)–O(11)	2.84(8)
O(11)–O(7B)	2.65(7)	O(11)–O(7A)	2.54(6)
O(7B)–O(6)	2.64(7)	O(7A)–O(6)	2.76(7)

correspond to the most inaccurate positions, O(7A) and O(13B), and are probably not significant. The framework "W_4O_{13}" bounds the pentagonal and hexagonal tunnels parallel to **c**, which are occupied by the thallium ions. In a pentagonal tunnel, each Tl(1) atom is surrounded by four oxygen atoms with distances ranging from 2.65 to 2.90 Å and three others located at about 3.06 Å. The other Tl(1)–0 are greater than 3.30 Å. In a hexagonal tunnel, the results obtained for the average structure enable us to propose two types of sites for the Tl(3) atom. When this atom is located in the nearest site of O(12), the five shortest distances found range from 3.01 to 3.16 Å. On the other hand, if it occupies the other site, the shortest distances observed range from 2.89 to 3.16 Å. Calculations on superstructure reflections did not allow a choice between

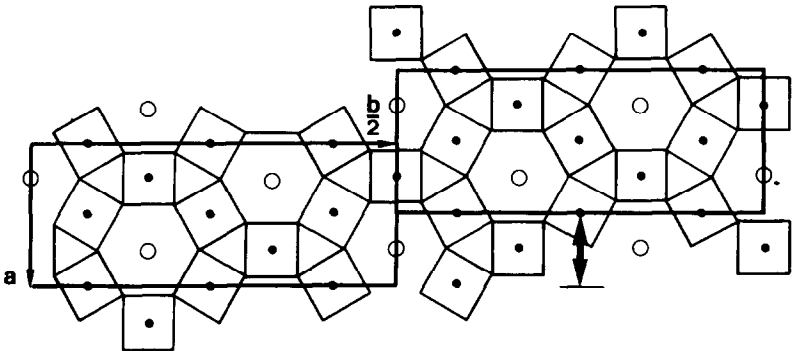

FIG. 4. Relationship between HTB and $Tl_2W_4O_{13}$ structures.

these two possibilities. In both cases, the Tl(3) is sited at a distance of 0.25 Å from the axis of the hexagonal tunnel.

Discussion and Conclusion

The $Tl_2W_4O_{13}$ structure is strongly related to that of the HTB as is confirmed by comparing Figs. 2 and 4. The octahedral framework is built up of HTB blocks, which extend to infinity in the **a** and **c** directions, with a width delimiting two rows of hexagonal tunnels along **b**. These blocks, which are shown as rectangles in Fig. 4, are displaced with respect to one another by $a/2$. In a first approximation, the $Tl_2W_4O_{13}$ structure can be deduced from the bronze structure by selectively removing some octahedra (Fig. 5a) and then shearing along **a**. The remaining HTB blocks then form pentagonal tunnels (Fig. 5b). The ideal structure so obtained would have a "b" parameter half of that observed. In fact, the framework is distorted and two successive HTB blocks are mirror images of each other in a "b" glide plane (001).

This model is in some respects analogous to that proposed by Steadman *et al.* (*8*) and Hussain and Kihlborg (*9*) for the bronzes Sn_xWO_3 and K_xWO_3, respectively. The host lattice of the latter can also be formed by the same selective elimination of some of the octahedra (Fig. 5a), but in the second step, the HTB blocks are directly shared by their corners (Fig. 5c), leading to the multiple phases described by Hussain and Kihlborg as intergrowths of WO_3 and HTB structures.

In a similar manner, variation of the width of the HTB blocks may be suggested here. The limit structure would have the composition $Tl_6B_{10}X_{34}$ (B being the metal and X the anion; X = O, F) and would be built up of HTB blocks, the width of which corresponds to one row of hexagonal tunnels only (Fig. 5d). A series of multiple phases with the

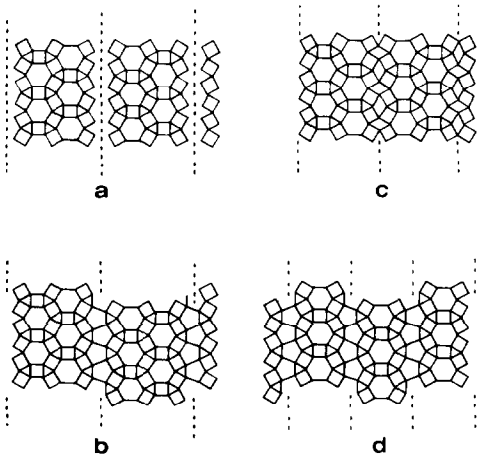

FIG. 5. Intergrowth mechanism. (a) HTB. Formation of blocks by selective removing of octahedra. (b) Lattice obtained after **a**/2 shear. (c) HTB blocks linked by corners sharing (K_xWO_3 from Hussain and Kihlborg). (d) The limit structure "$Tl_6B_{10}X_{34}$."

formula $(TlB_3X_9)_n \cdot Tl_6B_{10}X_{34}$ corresponding to the intergrowth of the HTB structure and of $Tl_6B_{10}X_{34}$ may thus be predicted. $Tl_2W_4O_{13}$ corresponds to $n = 2$ in this series.

On account of the interpolation nonstoichiometry observed in the HTB oxides, a double nonstoichiometry leading to the formula $(Tl_{1-x}B_3X_9)_n \cdot Tl_6B_{10}O_{34}$ may also be possible.

The presence of pentagonal tunnels as in tetragonal tungsten bronzes (*10*) should also be pointed out. Furthermore, this type of arrangement, which consists of edge-shared pentagonal tunnels forming ribbons, is relatively rare. It has, however, been observed in oxides of the Ta_2O_5–WO_3 system as described by Stephenson and Roth (*11*). Here the pentagonal tunnels are occupied by Ta–O chains.

References

1. B. RAVEAU, *Rev. Inorg. Chem.*, in press.
2. A. MAGNELI, *Acta Chem. Scand.* **7**, 315 (1953).
3. G. C. SHIVAHARE, *Naturwissenschaften*, 406 (1964).
4. C. MICHEL, Thèse de 3ème cycle, Caen (1971).
5. D. T. CROMER AND J. T. WABER, *Acta Crystallogr.* **18**, 104 (1965).
6. T. SUZUKI, *Acta Crystallogr.* **13**, 279 (1960).
7. D. T. CROMER, *Acta Crystallogr.* **18**, 17 (1965).
8. R. STEADMAN, R. J. D. TILLEY, AND I. J. MCCOLM, *J. Solid State Chem.* **4**, 199 (1972).
9. A. HUSSAIN AND L. KIHLBORG, *Acta Crystallogr. Sect. A* **32**, 551 (1976).
10. A. MAGNELI, *Ark. Kemi.* **1**, 213 (1949).
11. N. C. STEPHENSON AND R. S. ROTH, *Acta Crystallogr. Sect. B* **27**, 1010, I, II, III, IV, V (1971).